GHz-bandwidth Silicon Photonics Multichannel Filter for Super-Channel Transceiver

Yiwei Xie
Centre for Optical and Electromagnetic Research
State Key Laboratory for Modern Optical Instrumentation
Zhejiang University
Hangzhou, China.
xieyiw@zju.edu.cn

Hao Yan
Centre for Optical and Electromagnetic Research
State Key Laboratory for Modern Optical Instrumentation
Zhejiang University
Hangzhou, China
yanhao53@zju.edu.cn

Daoxin Dai
Centre for Optical and Electromagnetic Research
State Key Laboratory for Modern Optical Instrumentation
Zhejiang University
Hangzhou, China
dxdai@zju.edu.cn

***Abstract*—We propose and demonstrate a novel GHz-bandwidth multichannel optical filter (MOF) design using a resonator-assisted discrete-Fourier-transform interferometer topology. By employing ultra-low-loss silicon waveguides and low-phase-error phase-tuning elements, the present reconfigurable MOF is able to be implemented on silicon platform, which is challenge for realizing GHz-bandwidth filters due to the large waveguide propagation loss. In particular, the proposed MOF is capable of performing some specific filtering responses with e.g. near-rectangular shape as well as sinc shape. We successfully demonstrated the generation of WDM superchannel comprising four 10-Gaud subchannels using the designed MOF.**

Keywords-mutltichannel optical filter; Nyquist-wavelength division multiplexing; discrete Fourier transform circuit

I. INTRODUCTION

Due to the ever-increasing data traffic worldwide, multi-carrier (or super-channel) techniques are of high interest to increase the transmission capacity, as they support high spectrum utilization by allowing carriers to be spaced at or close to signal baud rate. For multi-carrier transceivers, multichannel optical filters (MOFs) that are able to shape the transmitted spectra to be only slightly wider than the signal baud rate, and allow carriers densely pack together are highly desirable [1].

Arrayed waveguide grating (AWG) has been widely used in multi-channel (de)multiplexing [2] thanks to the compact size. However, it suffers channel non-uniformity. Alternatively, discrete Fourier transform (DFT) circuits cooperating multi-arm nested Mach-Zehnder interferometer (MZI) have the advantages of channel uniformity, and also offer design freedom and easy incorporation of tuning elements for flexible N-WDM transceiver. In terms of super-channel MOF implementation, DFT circuits have been designed to combine with finite-impulse-response (FIR) filters [3], in which case one usually requires tens (even hundreds) of taps would be required to achieve a near-rectangular passband with a roll-off factor of < 10%. In contrast, infinite-impulse-response (IIR) filters using resonators has been demonstrated to work as a compact interleaver for Nyquist-wavelength division multiplexing (N-WDM) applications [4]. Thus, it is highly desirable to combine the DFT circuit and RAMZIs for the realization of super-channel MOFs [4].

In terms of integrated materials, most of the GHz-bandwidth WDM multiplexers have been reported on low-loss silica or silicon-nitride [5]. These filters usually have a large size of ~cm^2, and low thermo-tuning efficiency (~W/π), which limit their function extensions. Alternatively, silicon photonics has the advantages of high integrated density enabled by ultra-high index-contrast Δ and high TO coefficient as well as a high heat conductivity [6], it can support most of the optical devices and have the potential to realize fully-integrated reconfigurable WDM transceivers. However, it is very challenge for realizing GHz-bandwidth silicon filters (usually have centimeter-long delaylines) due to the large waveguide propagation loss.

In this work, we design a ring resonator-assisted discrete-Fourier-transform interferometer in a silicon platform to form scalable super-channel MOF using ultra-low-loss broadened photonic waveguides and phase-error-free tuning elements. The design can be configured to achieve a near-rectangular passband, roll-off factor of 8%, flat-top passband and scalable output ports. The demonstrated chip has a compact footprint of 2.14 mm^2 and an excess loss of ~6 dB. It has 16 heaters to control the filter passband shape. The present MOF has successfully implemented four channel 10-Gaud OOK-coded super-channel transmitter. This work shows great potential for next-generation high-capacity elastic optical communication networks.

II. DESIGN PRINCIPLE

Our MOF design consists of a multi-arm nested MZI followed by a resonator-assisted Mach-Zehnder interferometer (RAMZI). Figure 1(a) shows the circuit configuration with two resonators, four-tapped delaylines and four input ports, *n* as an example. The optical path differences, ΔL, of the delay lines is determined by the following equation: $\Delta L = c/(n\cdot \mathrm{FSR})$; here, c is the velocity of light and n is the effective index of the waveguides. The FSR is determined by product of the port count N, here $N = 4$, and the demultiplexing frequency spacing Δf. The following RAMZI circuit shapes the passband into near-rectangular response. Here the perimeter of the resonator is set as $c\cdot N\Delta t/n$, which determines the filtering bandwidth of the whole circuit.

The transfer function from the n-th input port to positions (i) and (ii) as follow [7]

$$H_n^{(\mathrm{i})}(z) = \sum_{m=0}^{1} a_m e^{-j2\pi m\cdot n/4}\cdot z^{-m}\frac{\sqrt{1-k_1}-e^{-j\theta_1}\cdot z^{-4}}{1-e^{-j\theta_1}\cdot z^{-N}\cdot\sqrt{1-k_1}} \quad (1)$$

$$H_n^{(\mathrm{ii})}(z) = \sum_{m=2}^{3} a_m e^{-j2\pi m\cdot n/4}\cdot z^{-m}\frac{\sqrt{1-k_2}-e^{-j\theta_2}\cdot z^{-4}}{1-e^{-j\theta_2}\cdot z^{-4}\cdot\sqrt{1-k_2}} \quad (2)$$

where k_1, k_2, and θ_1, θ_2 are the optical power coupling coefficient and the phase of the resonators in the RAMZI circuit. Finally, one has the output at position (iii) by combining the outputs at positions (i) and (ii). The value of phase shifters to perform DFT functions and the resonator's parameters to

achieve near-rectangular (Nyquist) filtering are also shown in Fig. 1(a).

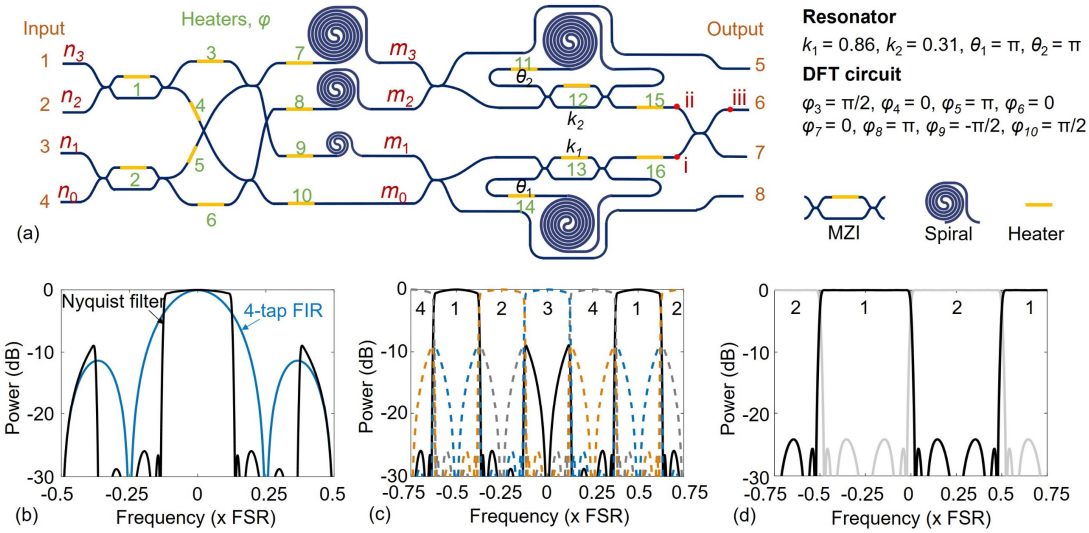

Fig.1. Our designed MOF: (a) Circuit configuration of the MOF. (b) The spectra of the MOF at output 6 when $k_{1,2}$ = 0 (4-tapped FIR filter) and optimum setting (Nyquist filter); (c) optimum settings for Nyquist MOF at four demultiplexing ports when m_0–$m_3 \neq 0$. (d) optimum settings for Nyquist MOF at two demultiplexing ports when m_0, m_2= 0 (or m_1, m_3 = 0) tuning the MZIs.

In this work, the delay length ΔL is approximately 2 mm for the FSR = 40 GHz, while the resonator perimeter is set as 8 mm, giving a passband bandwidth of 10 GHz compatible with the available opto-electro devices in the lab. To reduce the waveguide loss and chip area simultaneously, we use the design of a broadened Archimedean waveguide spiral with a tapered Euler-curve S-bend [8] for the delay lines as well as the resonators, as shown in Fig. 1(a). The silicon photonic waveguides are designed with a broadened core width of w_{co}= 2 μm to achieve a simulated ultra-low loss of 0.28 dB/cm. What's more, low-phase-error 2×2 thermo-optic MZIs with 2-μm-wide phase shifters (corresponding to Heaters 1,2,12,13) are employed for tuning the power distributions to reduce the power consumption and calibration complexity thanks to the advantages of negligible random phase errors due to the fabrication imperfection.

Figure 1(b)-1(d) show the theoretical transmission spectra of the MOF using Eqs. (1) and (2). When the power coupling ratio, k_1, k_2 set as *0*, the device is configured as a 4-tapped FIR filter with a sinc-like response, as shown in Fig. 1(b). With the parameter k and θ values as indicated in Fig. 1(a), each demultiplexing port has a near-rectangular passband with a stopband extinction of 25 dB and sharp transition bands as shown in Fig. 1(c). When tuning the heaters (φ_1, φ_2) in MZI, so that m_0, m_2= 0 (or m_1, m_3 = 0), the device is reduced to an interleaver, whose FSR and passband ratio (FPR) is 2. The corresponding transmission spectra for two demultiplexing ports is shown in Fig. 1(d).

III. Chip Characterization

The chip is fabricated on silicon-on-insulator (SOI) platform with a 220-nm-thick silicon core layer and a 2-μm-thick buried oxide (BOX) layer, and the footprint is 2.14 mm^2. The chip picture and the zoom-in pictures of key components are shown in Fig. 2(a). Eight optical ports (four inputs and four outputs) are placed on the left side of the chip for fiber array coupling. An adiabatic taper waveguide is used to connect the 500-nm-wide singlemode section with the 2-μm multimode spiral with a measured loss of 0.3 dB/cm. A compact silicon waveguide crossing with 10 mdB insertion loss is used in the DFT circuit section [9]. The low-phase-error MZI loss is measured as ~0.35 dB and the extinction ratios are >25 dB in a large bandwidth of >80 nm. All the heaters are led to one sides of the chip for wire-bonding to a printed circuit board (PCB), as shown in Fig. 2(b).

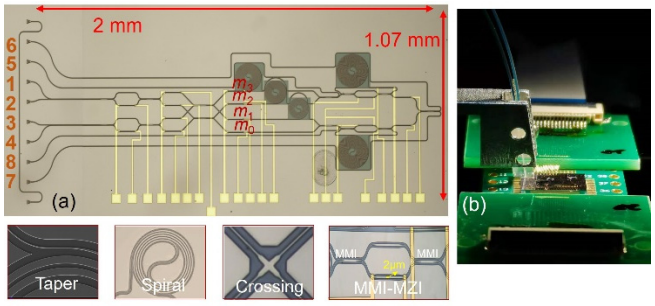

Fig. 2. (a) chip picture and zoom-in pictures of taper, delay line, crossing and MMI-based MZI; (c) a photo of the packaged chip.

Figure 3(a) shows the measured filter response when configured with the optimum setting. The measured results are in good agreement with the theoretical results (using Eqs. (1) and (2)) in Fig. 1(b), showing great excellence of the design as well as the fabrication. The slight deviation is due to the limited extinction ratio for the fabricated MZIs and heater crosstalk in the chip. The obtained passband has a 3-dB bandwidth of 10 GHz, and a 25-dB bandwidth of 10.8 GHz, showing a roll-factor as low as 8%. In Fig. 3(b), when the coupling coefficients, k_1, k_2 are set as 0 and all tap coefficients a_m to be equal, the response has a sinc-like shape. With the number the resonators (1, 2) involved, the spectra is shaped to achieve a near-rectangular shape with roll-off factor depends on the number of resonators. Figure 3(c) shows two filter shapes with FPR=2 and FPR=4, respectively, which is achieved by appropriately changing the tap amplitude coefficients controlled by heaters (φ_1, φ_2). Figure 3(d) shows the measured frequency responses of the device at four demultiplexer ports. It shows that all output ports have

near-rectangular responses with a channel spacing equal to the 3-dB bandwidth, allowing ultra-dense multiplexing (e.g., Nyquist-spacing multiplexing). These measurement results demonstrate the full programmability of the chip.

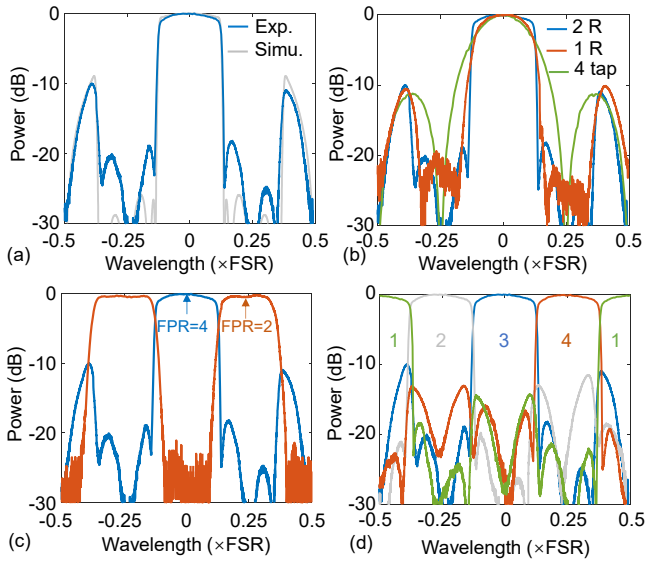

Fig. 3. Filter frequency response: (a) a comparison between measurement and theoretical single channel. Demonstrations of passband bandwidth variation with respect to (b) the number of rings; (c) variation of filter's FPR; and (d) frequency responses with four demultiplexing ports within one FSR (FSR= 40 GHz).

We test the MOF in a super-channel signals generation system, as shown in Fig. 4, in which we used four 40 GHz-spaced optical subchannel signals where each subchannel was modulated to a 10-Gbaud OOK signal generated by a bit error rate test (BERT) equipment, consistent with the MOF 3-dB bandwidth. The modulated signals were combined and shaped by the present MOF chip to generate super-channel signals comprising four 10-Gbaud OOK-modulated Nyquist subchannels. A waveshaper and a 40-GHz photodetector (Finisar XPDV3120) were used to detect the selected subchannel. The measured spectra of the optical signals, namely the original subchannel signals before the MOF chip in the transmitter, the filtered/multiplexed super-channel signal after the MOF, are shown in Fig. 4 (b) and 4(c). Figure 4(d) gives a comparison for the back-to-back optical signal to noise ratio (OSNR) performance of a single Nyquist signal and a demultiplexed subchannel (subchannel 2) of the super-channel signals. Subchannel 2 in the super-channel signals has a 0.6-dB reduction in the signal quality compared with the single Nyquist channel, due to the crosstalk from neighboring subchannels. As shown the eye diagrams in Fig. 4(c), our MOF performs sufficiently well in N-WDM systems.

IV. Conclusion

We developed an optical MOF for four 10-GHz-spaced subchannels using silicon technology with the help of low-loss broadened waveguides and low-phase-error MZIs. The MOF provides near-rectangular spectra response with roll-off factor of 8%, and a FSR is selectable. We successfully demonstrated super-channel signal generation with an OSNR penalty of 0.6 dB using the MOF chip and 10-Gbaud OOK subchannels. The results of this work show potential for realizing high-spectral-efficiency multi-carrier transceivers and ROADMs in a fully-integrated form.

Acknowledgment

This work was supported by Zhejiang Provincial Natural Science Foundation (LGF21F050003); National Natural Science Foundation of China (NSFC) (62175214, 61905209, 62111530147); Open Project of Advanced Laser Technology Laboratory of Anhui Province (AHL2021KF05).

References

[1] O. Gerstal, M. Jino, A. Lord, S. J. B. Yoo, "Elastic Optical Networking: A New Design Dawn for the Optical Layer?," IEEE Communication Magazine, vol. P. S12, Feb 2012.

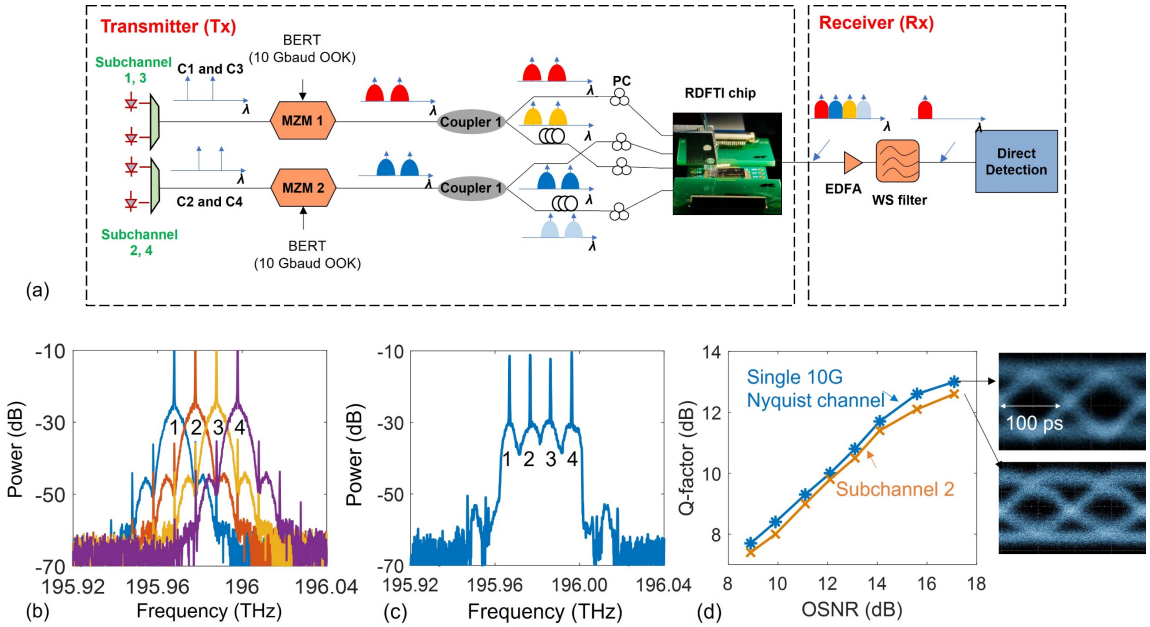

Fig. 4. Transmission characteristics measurement: (a) Setup for demonstrating super-channel signal generation. The measured optical signal spectra of the transmitted OOK signal (a) before and (c) after the MOF chip. (d) Measured Q-factor characteristics of second subchannel signal with ASE noise loading.

[2] D. Dai, J. Wang, S. Chen, S. Wang, and S. He, "Monolithically integrated 64-channel silicon hybrid demultiplexer enabling simultaneous wavelength-and mode-division-multiplexing," Laser Photonics Rev. vol. 9, pp. 339-344, May 2015.

[3] T. Goh, M. Itoh, H. Yamazaki, T. Saida, and T. Hashimoto, "Optical Nyquist-filtering multi/demultiplexer with PLC for 1-Tb/s class super-channel transceiver," in Optical Fiber Communication conference (OFC) and Exhibition (Optical Society of America), 2015, pp. Tu3A-5.

[4] L. Zhuang, C. Zhu, Y. Xie, M. Burla, C. G. Roeloffzen, M. Hoekman, B. Corcoran, and A. J. Lowery, "Nyquist-filtering (de) multiplexer using a ring resonator assisted interferometer circuit," J. Lightwave Technol., vol. 34, pp. 1732-1738, Apr 2016.

[5] C. G. Roeloffzen, M. Hoekman, E. J. Klein, L. S. Wevers, R. B. Timens, D. Marchenko, et al. "Low-loss Si3N4 TriPleX optical waveguides: Technology and applications overview," IEEE journal of selected topics in quantum electronics, vol. 24, pp. 1-21, Jan 2018.

[6] Y. Xie, Y. Shi, L. Liu, J. Wang, R. Priti, G. Zhang, et al. "Thermally-reconfigurable silicon photonic devices and circuits," IEEE Journal of Selected Topics in Quantum Electronics, vol. 26, pp. 1-20, Jun 2020.

[7] C. K. Madsen, and J. H. Zhao, Optical Filter Design and Analysis: A Signal Processing Approach, USA: Wiley, 1999.

[8] Y. Xie, S. Hong, H. Yan, C. Zhang, L. Zhang, L. Zhuang, and D. Dai, "Low-loss chip-scale programmable silicon photonic processor," Opto-Electronic Advances, vol. 6, pp. 220030-1, Mar 2023.

[9] Y. Peng, H, Li, and D. Dai, "Compact silicon photonic waveguide crossings with sub-10-mdB loss," Asia Communications and Photonics Conference, 2021, pp. T4A. 130.